Front. Earth Sci. 2023, 17(3): 752–759
https://doi.org/10.1007/s11707-022-1026-x

RESEARCH ARTICLE

Measurement of CO_2 adsorption capacity with respect to different pressure and temperature in sub-bituminous: implication for CO_2 geological sequestration

Sijian ZHENG (✉)[1,2], Shuxun SANG (✉)[1,2,3], Shiqi LIU[1,2], Meng WANG[1,2], Lutong CAO[4], Xin JIN[5], Guangjun FENG[3], Yi YANG[5]

1 Jiangsu Key Laboratory of Coal-based Greenhouse Gas Control and Utilization, China University of Mining and Technology, Xuzhou 221108, China
2 Carbon Neutrality Institute, China University of Mining and Technology, Xuzhou 221008, China
3 School of Resources and Geosciences, China University of Mining and Technology, Xuzhou 221116, China
4 China Coal Technology and Engineering Group Coal Mining Research Insitute, Beijing 100013, China
5 Xi'an Research Institute, China Coal Technology and Engineering Group, Xi'an 710077, China

Abstract CCUS (carbon capture, utilization, and storage) technology is regarded as a bottom method to achieve carbon neutrality globally. CO_2 storage in deep coal reservoirs serves as a feasible selection for CCUS, and its storage potential can be attributed to the CO_2 adsorption capacity of the coal. In this paper, a series of CO_2 adsorption isotherm experiments were performed at different pressures and temperatures in sub-bituminous coal from the southern Junggar Basin (reservoir temperature ~25.9°C and pressure ~3.91 MPa). In addition, the high-pressure CO_2 adsorption characteristics of the southern Junggar Basin coal were characterized using a supercritical D-R adsorption model. Finally, the CO_2 storage capacities in sub-bituminous coal under the *in situ* reservoir temperature and pressure were analyzed. Results indicated that the excess adsorption capacities increase gradually with increasing injection pressure before reaching an asymptotic maximum magnitude of ~34.55 cm^3/g. The supercritical D-R adsorption model is suitable for characterizing the excess/absolute CO_2 adsorption capacity, as shown by the high correlation coefficients > 0.99. The CO_2 adsorption capacity increases with declining temperature, indicating a negative effect of temperature on CO_2 geological sequestration. By analyzing the statistical relationships of the D-R adsorption fitting parameters with the reservoir temperature, a CO_2 adsorption capacity evolution model was established, which can be further used for predicting CO_2 sequestration potential at *in situ* reservoir conditions. CO_2 adsorption capacity slowly increases before reaching the critical CO_2 density, following a rapid decrease at depths greater than ~800 m in the southern Junngar Basin. The research results presented in this paper can provide guidance for evaluating CO_2 storage potential in deep coal seams.

Keywords CCUS, CO_2 adsorption capacity, pore structure, CO_2 geological sequestration, Junggar Basin

1 Introduction

CCUS (carbon capture, utilization, and storage) refers to the process of separating CO_2 from industrial processes or the atmosphere and then directly utilizing or injecting it into the stratum to achieve permanent CO_2 emission reduction (Andersen et al., 2020; Leflay et al., 2021; Zheng et al., 2022a). According to the International Energy Agency (IEA) sustainable development scenario goals, CCUS will achieve a 15% cumulative carbon emission reduction by 2070. The key technical links of CCUS include CO_2 geological storage potential evaluation, CO_2 emission sources investigation, and source-sink matching optimization (Fig. 1). Potential geological storage sites include depleted oil and gas reservoirs, deep brine layers, deep unrecoverable coal seams, shale reservoirs and so on (Huo et al., 2017; Zheng et al., 2020).

CO_2 storage in deep coal beds has a desirable dual benefit both in natural gas efficiency development and excess carbon reduction (Zhang et al., 2013; Sun et al.,

Received August 30, 2022; accepted October 10, 2022

E-mail: sijian.zheng@cumt.edu.cn (S. Zheng)
shxsang@cumt.edu.cn (S. Sang)

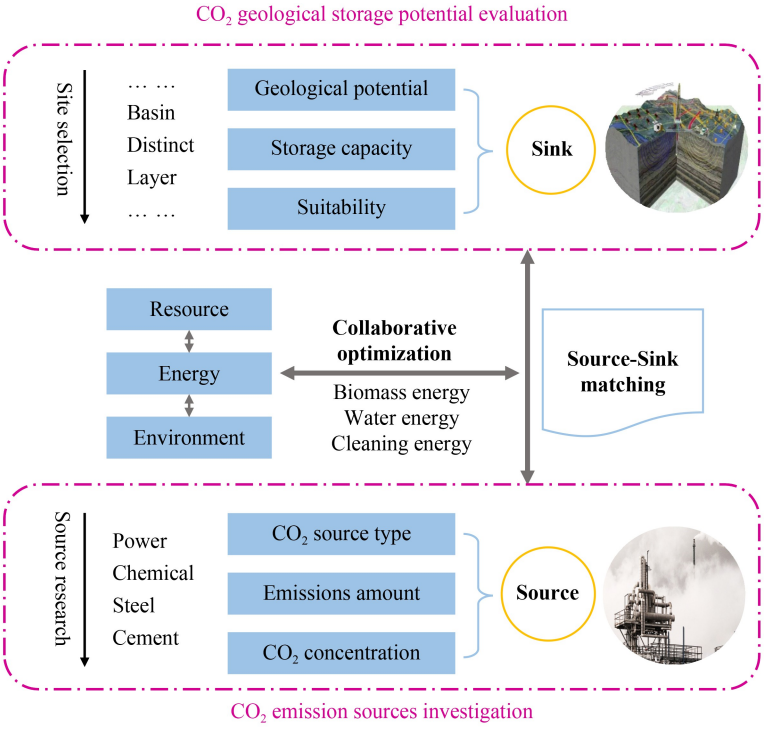

Fig. 1 Key technical links of the CCUS technology.

2018; Liu et al., 2019a). There are three main controlling factors in the CO_2 storage potential of coals (Han et al., 2019; Zhou et al., 2019; Zhou et al., 2021a). The first is the coal seam geological features, such as sedimentary environment, burial history, and tectonic development. The second is the *in situ* coal reservoir characteristics, such as porosity, permeability, and adsorption capacity. The third is on-site engineering construction, such as injection pressure and rate.

CO_2 adsorption capacity is essential in controlling the coal seam storage potential. The isothermal adsorption experiments are usually considered an essential tool for describing the adsorption behavior characteristics of coals (Liu et al., 2017; Zheng et al., 2018; Luo et al., 2019; Sun et al., 2021; Zhou et al., 2021b). With in-depth study of the six types of isothermal adsorption curves, adsorption theories to explain the curves have been successively developed, such as the Langmuir equation, BET equation, FHH equation, Kelvin equation, Polanyi theory, D-R model, and so on (Du et al., 2021; Shi et al., 2022; Liu et al., 2022).

Recently, the supercritical phase effect on the CO_2 adsorption behavior in coals continues to be widely studied (Perera et al., 2011; Wang et al., 2015; Dutka, 2019; Ma et al., 2022). The volumetric isotherm adsorption experiment results indicate that methane adsorption volume decreases supercritical CO_2 pretreatment (Zhou et al., 2018). Hui et al. (2019) performed gravimetric isotherm adsorption experiments to analyze the influence of supercritical CO_2 exposure on adsorption capacity. The experimental results indicated that the maximum CO_2 adsorption capacity declined as the supercritical phase gas treatment continued. Additionally, some literature has shown that after supercritical CO_2 treatment, the CO_2 adsorption capacity of coal and the overall adsorption heat decrease. Furthermore, the degree of CO_2 adsorption capacity decrease appears to be related to coal rank (Liu et al., 2019b; Zhang et al., 2019). It should be noted that few researchers have considered the effect of supercritical CO_2 adsorption volume on CO_2 storage capacity in coals. The inadequacy in CO_2 adsorption curves with respect to temperatures may contribute to an inaccurate evaluation of CO_2 storage capacity in coals.

In this paper, four temperatures (30°C, 45°C, 60°C, and 75°C) were chosen to characterize the CO_2 adsorption capacity of sub-bituminous coal taken from the southern Junggar Basin. Supercritical D-R adsorption theory was introduced for adsorption data fitting, and the temperature effect on adsorption capacity was estimated successively. Finally, an absolute/excess CO_2 adsorption capacity prediction model was established, which was used to estimate the CO_2 geological storage potential under *in situ* conditions – from the perspective of adsorbed phase.

2 Sampling and experiments

2.1 Samples

In this study, coal was obtained from a coal mine (depth ~400 m) in the southern Junggar Basin. The petro-

physical parameters are listed in Table 1. R_o and proximate analysis experiments were performed under the Chinese standard GB/T 6948-2008. The R_o of the selected coal values as ~0.53%, classifying it as sub-bituminous coal. The porosity (Φ) of the coal was measured using helium porosity experiments, following the Chinese standard GB/T 34533-2017. The helium-measured porosity of the coal was 6.43%, as shown in Table 1.

2.2 Pore structure characterization experiments

Low-temperature N_2 gas adsorption (LT-N_2GA) measurements were performed using a Micromeritics ASAP-2020 instrument, following the Chinese standard of SY/T6154-1995. For sample preparation, large-sized coals were crushed to 60−80 mesh, then dried at 110°C for 12 h in an oven to remove impurity gas and moisture. After sample drying, all coal powders were evacuated for complete outgassing in a high vacuum system for 5 h. Using N_2 gas with a purity of 99.99%, adsorption/desorption isotherms of coal powders were measured successively with the relative pressures (P/P_0) of 0.009–0.998 at a temperature of 77.4 K. Based on the N_2 adsorption branch, the Barrett-Joyner-Halenda (BJH) model and multi-point Brunauer-Emmett-Teller (BET) model were applied to calculate the pore volume and specific surface area, respectively (Yao et al., 2008).

NMR is a quick, non-destructive assessment of pore structure characterization (Liu et al., 2020; Zhou et al., 2020, 2022; Lin et al., 2021; Zhao et al., 2022). The workflow of the NMR experiments for pore structure characterization was as follows.

a) A standard-size core (radius ~12.5 mm, length ~ 50 mm) was drilled from the large lump of coal.

b) 72-h vacuum drying occurred and was sufficient to remove all the moisture in the coal cores.

c) Full water saturation of coal cores was obtained by using pressurized water extraction.

d) The NMR T_2 relaxation of coal cores was obtained using a Niumag-60 NMR apparatus. Note that the NMR parameters set in this study were the same as the previous study (Zheng et al., 2022b), with 0.3 ms echo spacing, 10000 echo numbers, and 64 repetition times.

2.3 High-pressure CO_2 adsorption measurements

In this study, high-pressure CO_2 adsorption isotherm measurements were performed by the volumetric method. The experimental CO_2 excess adsorption capacities were estimated based on the ideal gas equation of state. The CO_2 adsorption amount of the coal sample is the difference between the total injected gas amount and the free gas amount in the cells. First, the coal powder (with a size of 60−80 mesh) underwent dry treatment for 72-h at a temperature of 110°C before the experiment to remove moisture. Then, the high-pressure CO_2 adsorption isotherm measurements were performed by following the Chinese standard GB/T 19560-2008. Four temperatures of 30°C, 45°C, 60°C, and 75°C were chosen to characterize the CO_2 adsorption capacity of sub-bituminous coal.

The CO_2 adsorption capacities direct estimates from adsorption isotherm measurements were defined as the Gibbs adsorption equation. The D-R adsorption model is often used for supercritical CO_2 adsorption capacity characterization (Sakurovs et al., 2007). The D-R model is expressed follows:

$$n_{ex} = n_0\left(1-\frac{\rho_g}{\rho_a}\right)\exp\left[-D\left(\ln\frac{\rho_a}{\rho_g}\right)^2\right]+k\rho_g, \quad (1)$$

where n_{ex} is the excess adsorption capacity, cm^3/g; n_0 is the maximum adsorption capacity, cm^3/g; D is the affinity coefficient of coal-CO_2; ρ_g is the density of the free phase CO_2, g/cm^3; ρ_a is the density of the adsorbed phase CO_2, set as 1.0 g/cm^3 (Day et al., 2008); k is the correction coefficient due to the CO_2 swelling-adsorption. The density of free phase CO_2 under specific conditions was directly estimated from the Physical Property Calculation Query platform. In addition, the absolute adsorption capacity of CO_2 (n_{ab}) for typical coal was calculated as follows:

$$n_{ab} = \frac{n_{ex}}{1-\frac{\rho_g}{\rho_a}}. \quad (2)$$

3 Results and discussion

3.1 Pore structure characterization of coal

Figure 2(a) presents the LT-N_2GA experimental curves of the coal. Based on the isotherm adsorption curve classification described in IUPAC, the adsorption/desorp-

Table 1 Detailed petrophysical information of the selected coals

Φ/%	R_o/%	Maceral composition/%				Proximate analysis/%			
		V	I	E	M	M_{ad}	A_d	V_d	FC_d
6.43	0.53	73.1	20.4	6.5	0	7.63	21.31	22.54	48.52

Notes: R_o is the maximum vitrinite reflectance under oil immersion; V is vitrinite content; I is inertinite content; E is exinite content; M is minerals content; M_{ad} is moisture (air-dried basis); A_d is ash (dry basis); V_d is volatile (dry, ash free basis); FC_d is carbon (air-dried basis).

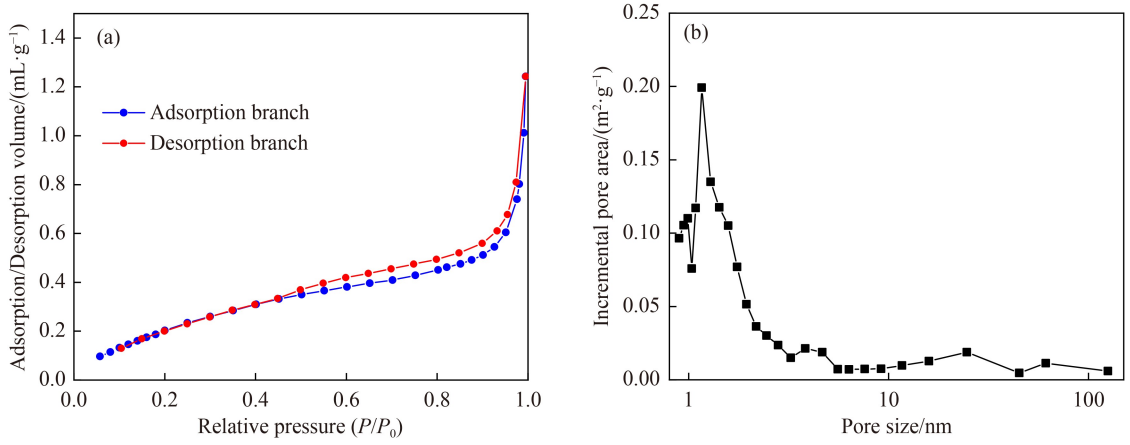

Fig. 2 Experimental results of the LT-N_2GA measurements.

tion curves in the studied coal as classified as H3. In the curves, the adsorption branch slowly rose when the relative pressure < 0.9 but rapidly increased in the relative pressure range of 0.9−1.0, with a weak hysteresis loop at approximately P/P_0 ~0.5. The typical adsorption/desorption curves of the coal indicate a pore morphology of open plate-like pores. The LT-N_2GA BET surface area and BJH pore volume calculated values were 1.428 m^2/g, and 2.274×10^{-3} cm^3/g, respectively.

As shown in Fig. 2(b), the surface area distribution of the coal exhibited a significant peak at approximately 1–2 nm, indicating the primary development of pores ranging in size from 1 to 2 nm. LT-N2GA experimental results suggest a significant contribution to the surface area from the micro-pores, as obtained from N_2 vapor adsorption at 273 K. The T_2 spectrum of the selected coal under full water saturation is shown in Fig. 3, exhibiting three distinct spectra peaks. For left-to-right, the peaks located at < 5 ms, 20−200 ms, and > 200 ms correspond to adsorption pores, seepage pores, and fractures, respectively – based upon the NMR pore size classification in Zheng et al. (2019).

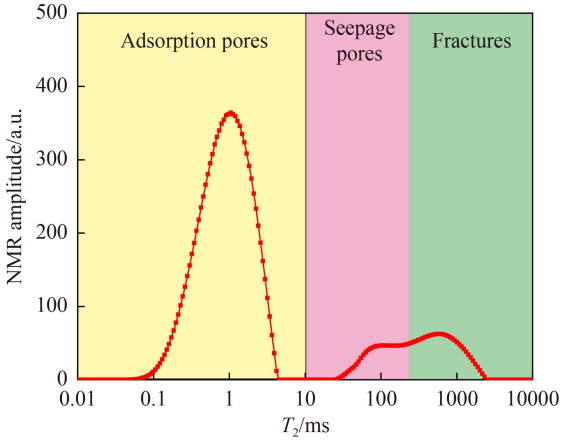

Fig. 3 NMR T_2 characterization of the water-saturated coal sample.

3.2 CO_2 isothermal adsorption of coal

Figure 4 represents the high-pressure CO_2 adsorption data for different temperatures. Results show that the excess CO_2 adsorption capacity was at its maximum values in the pressure range of 6−8 MPa under specified temperature conditions. After that, the excess CO_2 adsorption capacity decreased with pressure increase. Note that the maximum excess CO_2 adsorption capacity gradually decreased with temperature increase.

Taking 30°C high-pressure CO_2 adsorption results as an example, the maximum excess adsorption capacity was ~34.55 cm^3/g. The CO_2 excess adsorption amount increased gradually with the injection pressure before reaching an asymptotic maximum magnitude of ~34.55 cm^3/g. After that, the curves present irregular descents: the first represents a rapid drop from 6 to 10 MPa and then follows a long adsorption tail. Note that the descents had different pressures where the tail formed at different temperatures. In addition, the excess adsorption capacity decreased with temperature at a relatively low-pressure range. Conversely, the higher temperature indicates a

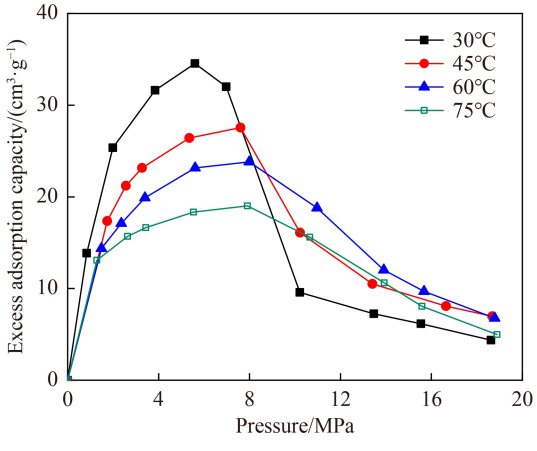

Fig. 4 Experimental results of CO_2 isothermal adsorption concerning different temperatures.

greater excess adsorption capacity within a high pressure scenario.

This paper used the free phase density instead of the equilibrium pressure to fit the supercritical CO_2 adsorption data, creating D-R adsorption model. An essential first step in D-R adsorption model fitting is determining the free-phase CO_2 density under specific pressures and temperatures. The estimated free CO_2 densities in this paper are listed in Table 2. By introducing Eq. (1), the fitting relationship between excess adsorption capacity and free CO_2 densities was displayed is Fig. 5.

The curves exhibit two distinct trends: the first represents a rapid increase in the CO_2 density of 0−0.2 g/cm^3, following a quick decline. Compared with the excess adsorption curves in Fig. 4, the excess adsorption capacity under every experimental point declined with increasing temperature. In addition, the excess adsorption curves at different temperatures show no intersections.

The fitting results of the D-R adsorption model are listed in Table 3. Fitting results show that all correlation coefficients are greater than 0.99, indicating that the D-R adsorption model can accurately describe the gaseous to supercritical CO_2 adsorption characteristics in sub-bituminous coal. In the 30°C–75°C temperature range, the maximum adsorption capacity n_0 ranged from 51.725 to 27.651 cm^3/g, D ranged from 0.048 to 0.068, and k ranged from −2.096–−10.902.

The relationships between the D-R adsorption model fitting parameter *vs*. temperature are displayed in Fig. 6. n_0 shows a statistically significant positive linear relationship with the reciprocal of temperature (R^2 ~0.9798). A linear fit to the relationship of D to temperature to the 2 photons yielded the relationship between temperature and D. In addition, k shows a statistically significant positive linear relationship with experimental temperature, with a high correlation coefficient ~0.9810. The exceptional linear relationships between the experimental temperature and the supercritical D-R adsorption model fitting parameters indicate the reliability of the modified Eq. (1).

3.3 CO_2 adsorption capacity of the southern Junggar Basin

As discussed in Section 3.2, the supercritical D-R adsorption model fitting parameters exhibit highly significant linear relationships with reservoir temperature. Thus, it is acceptable to use the temperature parameter instead of other parameters such as maximum adsorption capacity n_0, D, and k, to describe Eq. (1). By integrating the expressions in Fig. 6 with the supercritical D-R adsorption model, Eq. (1) can be rewritten as

$$n_{ex} = \left(54091\frac{1}{T} - 127.57\right)\left(1 - \frac{\rho_g}{\rho_a}\right) \times \exp\left[-\left(\frac{0.0013T^2}{1000} - 0.073\right)\left(\ln\frac{\rho_a}{\rho_g}\right)^2\right] + (-0.1977T + 58.326)\rho_g. \quad (3)$$

To estimate the CO_2 adsorption capacity in the southern Junggar Basin with respect to reservoir depth, the first essential step is to estimate the free phase CO_2 densities under reservoir conditions. In this study, the geological conditions were assumed as 1) a geothermal gradient of 20°C/km and reservoir pressure gradient of 9.78 MPa/km (Liu et al., 2022); 2) sub-bituminous coal whose adsorption characteristics can be represented by the experimental coal sample in this paper; 3) water saturation was not considered. First, the temperatures and pressures at different depths were calculated based on the geothermal and pressure gradients, respectively. In addition, CO_2 density curves at depth were obtained from the Physical Property Calculation Query. Finally, the absolute adsorption capacity changes of sub-bituminous coal under *in situ* reservoir temperature and pressure were estimated based on Eq. (3).

The changing characteristics of CO_2 density over reservoir depth are shown in Fig. 7. The CO_2 density increased monotonically before reaching a critical point,

Table 2 Free CO_2 density under studied temperature and pressure

30°C		45°C		60°C		75°C	
Pressure/MPa	Density/(g·cm^{-3})	Pressure/MPa	Density/(g·cm^{-3})	Pressure/MPa	Density/(g·cm^{-3})	Pressure/MPa	Density/(g·cm^{-3})
0.84	0.02	1.74	0.03	1.49	0.02	1.29	0.02
1.99	0.04	2.56	0.05	2.36	0.04	2.64	0.04
3.85	0.09	3.27	0.06	3.40	0.06	3.44	0.06
5.6	0.15	5.36	0.12	5.61	0.11	5.54	0.10
6.98	0.26	7.61	0.22	7.99	0.19	7.91	0.16
10.21	0.78	10.22	0.53	10.97	0.36	10.65	0.26
13.47	0.83	13.41	0.71	13.91	0.56	13.93	0.41
15.54	0.85	16.64	0.77	15.67	0.63	15.59	0.49

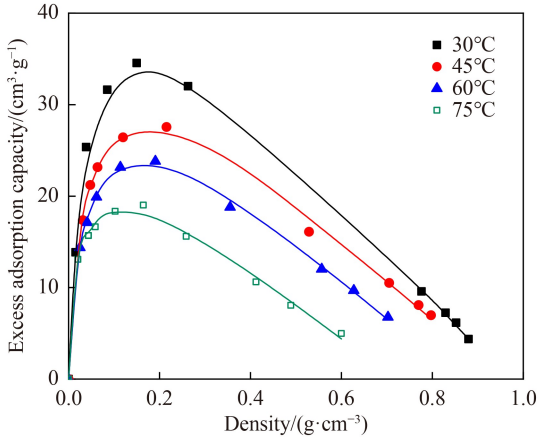

Fig. 5 Fitting curves between excess adsorption capacity and free CO_2 densities by supercritical D-R adsorption model.

Table 3 Supercritical D-R adsorption model fitting results of the coal

Parameter	30°C	45°C	60°C	75°C
n_0	51.725	40.492	36.018	27.651
D	0.048	0.065	0.076	0.088
k	−2.096	−3.981	−7.215	−10.902
R^2	0.992	0.993	0.995	0.991

and then increased slowly until reaching an asymptotic maximum magnitude. After calculating the CO_2 density curve, Eq. (1) and Eq. (3) were combined to estimate the absolute adsorption capacity of sub-bituminous coal under reservoir conditions in the southern Junggar Basin, which is shown in Fig. 8. Simulation results indicate the absolute CO_2 adsorption capacity first increased then declined with burial depth. Han et al. (2019) explained the changes in the absolute CO_2 adsorption capacity with burial depth mainly because of the CO_2 phase change. CO_2 adsorption capacity has a strong link with CO_2 density, suggesting that supercritical adsorption behavior on coals may be related to density variation.

4 Conclusions

In this study, four temperatures of 30°C, 45°C, 60°C, and 75°C were chosen to investigate the CO_2 adsorption capacity of sub-bituminous and CO_2 sequestration potential of the southern Junggar Basin. The main conclusions are as follows.

1) The pore structure of the sub-bituminous is characterized by adsorption pores, with the T_2 relaxation ranging from 0.1 to 2.0 ms. Low-temperature nitrogen adsorption/desorption curves indicate a pore morphology of open plate-like pores.

2) The excess adsorption capacity increases gradually with the injection pressure before reaching an asymptotic maximum magnitude of ~34.55 cm^3/g. The supercritical

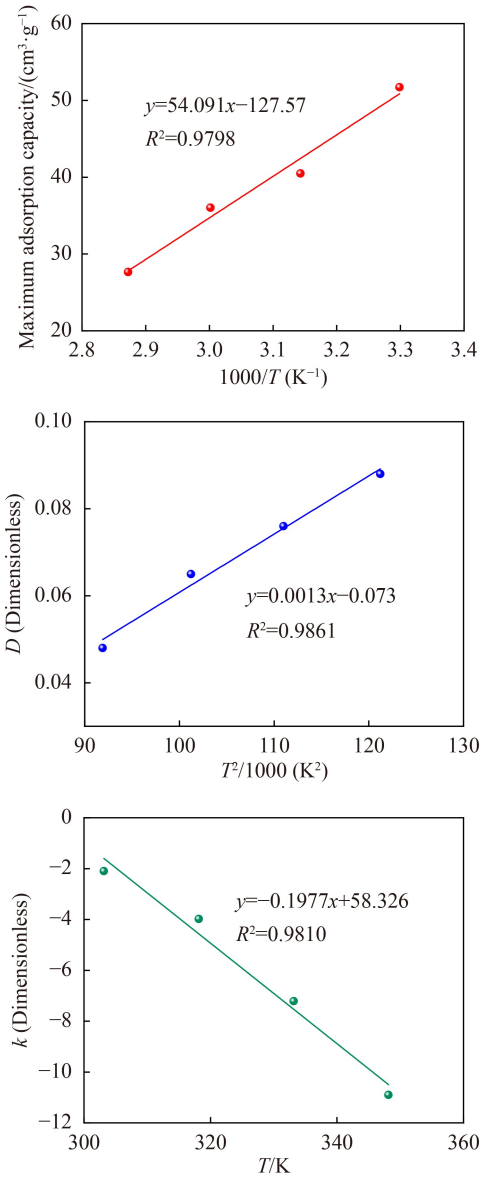

Fig. 6 The relationships between D-R adsorption model fitting parameter *vs.* temperature.

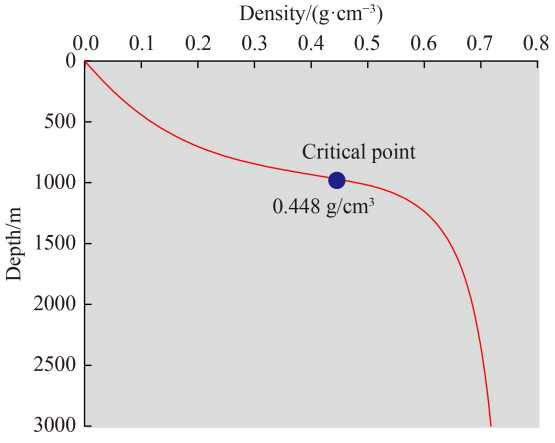

Fig. 7 The relationships of CO_2 density with reservoir depth.

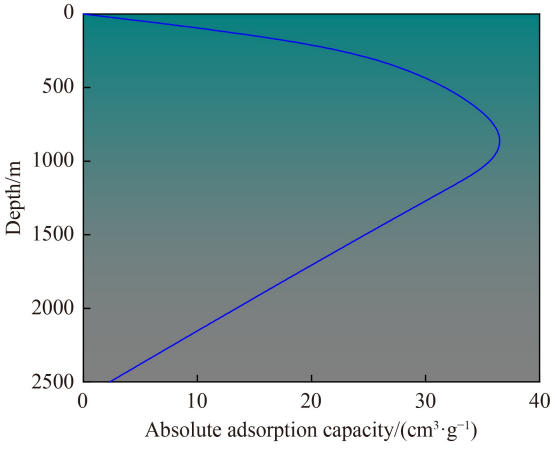

Fig. 8 Variation of absolute CO_2 adsorption capacities of sub-bituminous coal at reservoir temperatures and pressures in the southern Junggar Basin.

D-R adsorption model is suitable for characterizing the excess/absolute CO_2 adsorption capacity, as evident by the high correlation coefficients > 0.99.

3) The CO_2 adsorption capacity of the coal decreases with increasing temperature. CO_2 adsorption capacity increases at a lower rate before reaching the critical CO_2 density, following a decreasing trend at depths greater than ~800 m in the southern Junngar Basin.

Acknowledgments We acknowledge financial support from the National Natural Science Foundation of China (Grant Nos. 42141012, 41972168, and 42030810), the Peng Cheng Shang Xue Education Fund of CUMT Education Development Foundation (No. PCSX202204), the Fundamental Research Funds for the Central Universities (No. 2020ZDPYZD01) and a project funded by the Priority Academic Program Development of Jiangsu Higher Education Institutions.

References

Andersen P Q, Brattekås B, Zhou Y, Nadeau P, Nermoen A, Yu Z, Fjelde I, Oelkers E (2020). Carbon capture utilization and storage (CCUS) in tight gas and oil reservoirs. J Nat Gas Sci Eng, 81: 103458

Day S, Duffy G, Sakurovs R, Weir S (2008). Effect of coal properties on CO_2 sorption capacity under supercritical conditions. Int J Greenh Gas Control, 2(3): 342–352

Du X D, Cheng Y G, Liu Z J, Yin H, Wu T F, Huo L, Shu G X (2021). CO_2 and CH_4 adsorption on different rank coals: a thermodynamics study of surface potential, Gibbs free energy change and entropy loss. Fuel, 283: 118886

Dutka B (2019). CO_2 and CH_4 sorption properties of granular coal briquettes under *in situ* states. Fuel, 247: 228–236

Han S J, Sang S X, Liang J J, Zhang J C (2019). Supercritical CO_2 adsorption in a simulated deep coal reservoir environment, implications for geological storage of CO_2 in deep coals in the southern Qinshui Basin, China. Energy Sci Eng, 7(2): 488–503

Hui D, Pan Y, Luo P Y, Zhang Y, Sun L, Lin C (2019). Effect of supercritical CO_2 exposure on the high-pressure CO_2 adsorption performance of shales. Fuel, 247: 57–66

Huo P L, Zhang D F, Yang Z, Li W, Zhang J, Jia S Q (2017). CO_2 geological sequestration: displacement behavior of shale gas methane by carbon dioxide injection. Int J Greenh Gas Control, 66: 48–59

Leflay H, Pandhal J, Brown S (2021). Direct measurements of CO_2 capture are essential to assess the technical and economic potential of algal-CCUS. J CO_2 Util, 52: 101657

Lin T F, Liu X, Zhang J Y, Bai Y F, Liu J, Zhang Y P, Zhao Y, Cheng X, Lv J, Yang H (2021). Characterization of multi-component and multi-phase fluids in the Upper Cretaceous oil shale from the Songliao Basin (NE China) using T_1–T_2 NMR correlation maps. Petrol Sci Technol, 39(23–24): 1060–1070

Liu C J, Sang S X, Zhang K, Song F, Wang H W, Fan X F (2019b). Effects of temperature and pressure on pore morphology of different rank coals: implications for CO_2 geological storage. J CO_2 Util, 34: 343–352

Liu D M, Yao Y B, Chang Y H (2022). Measurement of adsorption phase densities with respect to different pressure: potential application for determination of free and adsorbed methane in coalbed methane reservoir. Chem Eng J, 446: 137103

Liu J, Xie L Z, Yao Y B, Gan Q, Zhao P, Du L H (2019a). Preliminary study of influence factors and estimation model of the enhanced gas recovery stimulated by carbon dioxide utilization in shale. ACS Sustain Chem & Eng, 7(24): 20114–20125

Liu J, Yao Y B, Liu D M, Elsworth D (2017). Experimental evaluation of CO_2 enhanced recovery of adsorbed-gas from shale. Int J Coal Geol, 179: 211–218

Liu X, Zhang J Y, Bai Y F, Zhang Y P, Zhao Y, Cheng X Y, Lv J C, Yang H, Liu J (2020). Pore structure petrophysical characterization of the Upper Cretaceous oil shale from the Songliao Basin (NE China) using low-field NMR. J Spectrosc, 2020: 9067684

Luo C J, Zhang D F, Lun Z M, Zhao C P, Wang H T, Pan Z J, Li Y H, Zhang J, Jia S Q (2019). Displacement behaviors of adsorbed coalbed methane on coals by injection of SO_2/CO_2 binary mixture. Fuel, 247: 356–367

Ma R Y, Yao Y B, Wang M, Dai X G, Li A H (2022). CH_4 and CO_2 adsorption characteristics of low-rank coals containing water: an experimental and comparative study. Nat Resour Res, 31(2): 993–1009

Perera M S A, Ranjith P G, Choi S K, Airey D (2011). The effects of sub-critical and super-critical carbon dioxide adsorption-induced coal matrix swelling on the permeability of naturally fractured black coal. Energy, 36(11): 6442–6450

Sakurovs R, Day S, Weir S, Duffy G (2007). Application of a modified Dubinin-Radushkevich equation to adsorption of gases by coals under supercritical conditions. Energy Fuels, 21(2): 992–997

Shi Q M, Cui S D, Wang S M, Mi Y C, Sun Q, Wang S Q, Shi C Y, Yu J Z (2022). Experiment study on CO_2 adsorption performance of thermal treated coal: inspiration for CO_2 storage after underground coal thermal treatment. Energy, 254: 124392

Sun X X, Yao Y B, Liu D M (2021). The behavior and efficiency of methane displaced by CO_2 in different coals and experimental conditions. J Nat Gas Sci Eng, 93: 104032

Sun X X, Yao Y B, Liu D M, Zhou Y F (2018). Investigations of CO_2-water wettability of coal: NMR relaxation method. Int J Coal Geol, 188: 38–50

Wang Q Q, Zhang D F, Wang H H, Jiang W P, Wu X P, Yang J, Huo P L (2015). Influence of CO_2 exposure on high-pressure methane and CO_2 adsorption on various rank coals: implications for CO_2 sequestration in coal seams. Energy Fuels, 29(6): 3785–3795

Yao Y B, Liu D M, Tang D Z, Tang S H, Huang W H (2008). Fractal characterization of adsorption-pores of coals from north China: an investigation on CH_4 adsorption capacity of coals. Int J Coal Geol, 73(1): 27–42

Zhang D F, Gu L L, Li S G, Lian P C, Tao J (2013). Interactions of supercritical CO_2 with coal. Energy Fuels, 27(1): 387–393

Zhang D F, Li C, Zhang J, Lun Z M, Jia S Q, Luo G J, Jiang W P (2019). Influences of dynamic entrainer-blended supercritical CO_2 fluid exposure on high-pressure methane adsorption on coals. J Nat Gas Sci Eng, 66: 180–191

Zhao P, He B, Zhang B, Liu J (2022). Porosity of gas shale: Is the NMR-based measurement reliable? Petrol Sci, 19(2): 509–517

Zheng S J, Sang S X, Yao Y B, Liu D M, Liu S Q, Wang M, Feng G J (2022b). A multifractal-based method for determination NMR dual T_2 cutoffs in coals. J Petrol Sci Eng, 214: 110488

Zheng S J, Yao Y B, Elsworth D, Liu D M, Cai Y D (2020). Dynamic fluid interactions during CO_2-ECBM and CO_2 sequestration in coal seams. Part 2: CO_2-H_2O wettability. Fuel, 279: 118560

Zheng S J, Yao Y B, Liu D M, Cai Y D, Liu Y (2018). Characterizations of full-scale pore size distribution, porosity and permeability of coals: a novel methodology by nuclear magnetic resonance and fractal analysis theory. Int J Coal Geol, 196: 148–158

Zheng S J, Yao Y B, Liu D M, Cai Y D, Liu Y (2019). Nuclear magnetic resonance surface relaxivity of coals. Int J Coal Geol, 205: 1–13

Zheng Y W, Gao L, Li S, Wang D (2022a). A comprehensive evaluation model for full-chain CCUS performance based on the analytic hierarchy process method. Energy, 239: 122033

Zhou J P, Xie S, Jiang Y D, Xian X F, Liu Q L, Lu Z H, Lyu Q (2018). Influence of supercritical CO_2 exposure on CH_4 and CO_2 adsorption behaviors of shale: implications for CO_2 sequestration. Energy Fuels, 32(5): 6073–6089

Zhou S D, Liu D M, Cai Y D, Wang Y J, Yan D T (2021b). Mineral characteristics of low-rank coal and the effects on the micro- and nanoscale pore-fractures: a case study from the Zhundong Coalfield, Northwest China. J Nanosci Nanotechnol, 21(1): 460–471

Zhou S D, Liu D M, Karpyn Z T, Cai Y D, Yao Y B (2021a). Dual compressibility characteristics of lignite, subbituminous, and high-volatile bituminous coals: a new insight into permeability. Transp Porous Media, 136(1): 295–317

Zhou S D, Wang H, Jiang S R, Yan D T, Liu D M, Zhang Z Y, Li G Q (2022). A novel approach to obtain fractal dimension in coals by LFNMR: insights from the T_2 peak and T_2 geometric mean. J Energy Eng, 148(3): 04022009

Zhou S D, Yan D T, Tang J G, Pan Z J (2020). Abrupt change of pore system in lacustrine shales at oil- and gas-maturity during catagenesis. Int J Coal Geol, 228: 103557

Zhou Y B, Li Z H, Zhang R L, Wang G Z, Yu H, Sun G Z, Chen L (2019). CO_2 injection in coal: advantages and influences of temperature and pressure. Fuel, 236: 493–500